y_m = amount of adsorbate which may be adsorbed in a monolayer on catalyst surface, moles/g. catalyst

Z = distance along reactor length, cm.

Greek Letters

δ = increase in the total number of moles in the system per mole of substance A reacted $= [(r + s + \ldots) - (a + b + \ldots)]/a$ for reaction $aA + bB + \ldots = rR + sS + \ldots$

ϵ = void fraction of packed section of the reactor, dimensionless

$\theta_A, \theta_W, \theta_E$ = fraction of catalyst monolayer covered with ethanol, water, and ether, respectively, dimensionless

θ_V = fraction of vacant catalyst sites in monolayer, dimensionless

$\kappa_A, \kappa_W, \kappa_E$ = adsorption rate coefficients for ethanol, water, and ether, respectively, moles/min. g. cat. atm.

$\kappa_{-A}, \kappa_{-W}, \kappa_{-E}$ = desorption rate coefficients for ethanol, water, and ether, respectively, moles/min. g. cat.

ρ_A, ρ_W, ρ_E = rate of adsorption of ethanol, water, and ether, respectively, moles/min. g. cat.

ρ_c = bulk catalyst density, g. cat./cc. reactor

ρ_M = molar density $= P/RT$, moles/cc.

ρ_{vA} = density of liquid ethanol feed, g./cc.

LITERATURE CITED

1. Acrivos, Andreas, *Ind. Eng. Chem.*, **48**, 703 (1956).
2. Arden, B. W., "An Introduction to Digital Computing," pp. 274-283, Addison Wesley, Reading, Massachusetts (1963).
3. Beek, John, "Advances in Chemical Engineering," Vol. 3, Academic Press, New York (1962).
4. Crider, J. E., and A. S. Foss, *AIChE J.*, **12**, 514 (1966).
5. Foss, A. S., *Chem. Eng. Prog. Symp. Ser. No. 25*, **55**, 47 (1959).
6. Kabel, R. L., Ph.D. thesis, Univ. Washington, Seattle, (1961).
7. ———, and L. N. Johanson, *AIChE J.*, **8**, 621 (1962).
8. ————————, *J. Chem. Eng. Data*, **6**, 496 (1961).
9. Lapidus, Leon, *Chem. Eng. Prog. Symp. Ser. No. 36*, **57**, 34 (1961).
10. Lehr, C. G., MS thesis, Pennsylvania State Univ., University Park (1966).
11. McGuire, M. L., and Leon Lapidus, *AIChE J.*, **11**, 85 (1965).
12. Mullarkey, T. B., MS thesis, Pennsylvania State Univ., University Park, in progress.
13. Wilhelm, R. H., *Pure Appl. Chem.*, **5**, 403 (1962).
14. Yamas, J. L., B.S. thesis, Pennsylvania State Univ., University Park (1964).
15. Yurchak, Sergei, B.S. thesis, ibid. (1964).

Manuscript received January 26, 1967; revision received October 26, 1967; paper accepted October 27, 1967. Paper presented at AIChE Houston meeting.

Stability of Adiabatic Packed Bed Reactors:

Effect of flow variations and coupling between the particles.

JOHN W. VANDERVEEN, DAN LUSS, and NEAL R. AMUNDSON

University of Minnesota, Minneapolis, Minnesota

A simple cell model is used for the determination of necessary and sufficient conditions for the stability of an adiabatic fixed bed reactor. These conditions are stronger than those obtained by considering only a perturbation of a single particle. Because of the nonuniqueness of the steady state profiles certain pathological effects can occur when the flow rate of the reactant is changed. Geometric coupling between the particles and heat transfer by radiation give rise to further complexities. Examples are given in which the trends predicted by the models have been observed experimentally by Wicke and Frank-Kamenetskii.

In the last decade a great deal of effort has been expended in an attempt to characterize the behavior of fixed bed reactors. This problem is of practical importance since an increasing number of industrially important reactions are carried out in fixed and moving beds, and a number of papers dealing with both theoretical and experimental results have appeared.

This study is based on earlier work (5) in which a simple continuous model of an adiabatic reactor with the reaction $A \rightarrow B$ showed the significance of the transient behavior of the bed. It was demonstrated that each catalyst pellet could, under suitable conditions, exist in

John W. Vanderveen is with Phillips Petroleum Company, Bartlesville, Oklahoma, and Dan Luss is at the University of Houston, Houston, Texas.

either of two stable states. As a consequence, the steady state temperature and concentration profiles for the bed were not uniquely specified by the steady state equations. This analysis was extended to cover the nonadiabatic case (6) and the case in which there is extensive back mixing (7) as characterized by a Fickian model.

Deans and Lapidus (2) described fixed beds by an array of two dimensional mixing cells. The advantage of this model is that it reduces the time of computation especially if one includes the effect of axial and intraparticle diffusion. McGuire and Lapidus (8) used such a model to investigate numerically the transient behavior of a catalytic reactor. Much machine time was required for the transient computations, and it was found that the system is strongly model dependent.

In this work a simple cell model will be used to describe the behavior of fixed beds by neglecting the effect of radial mixing. The model will enable us to determine necessary and sufficient conditions for the stability of the whole bed. These conditions are stronger than those deveeloped in (5) in which the effect of transient changes in the reacting phase was not included in the analysis. A simple graphical marching technique is developed which enables one to determine the temperature profiles in the bed for the case of simple reaction kinetics. The transient computations show some interesting effects when the flow rate of the reactants is changed. Some of these trends have been observed experimentally by Wicke and coworkers (9 to 12). Refined models with more coupling between the cells are investigated and compared with the simple model.

SIMPLE UNCOUPLED CELL MODEL

This model assumes the bed to be composed of a series of layers of cells, the cells being connected by the interstitial fluid stream. A schematic description of cell j is given in Figure 1. The thickness of each cell, ηD_p, depends on the structure of the bed. Most computations were done for a rhombohedral arrangement for which $\eta = \sqrt{2/3}$. The reaction is assumed to be first-order and irreversible, $A \rightarrow B$. The same notation as in the previous papers (5 to 7) will be used.

The mass and heat conservation equations for the fluid and the particle in cell j are

$$M(p_{j-1} - p_j) - (p_j - p_{pj}) = a_1 \frac{dp_j}{d\theta} \tag{1}$$

$$H(t_{j-1} - t_j) - (t_j - t_{pj}) = a_2 \frac{dt_j}{d\theta} \tag{2}$$

$$p_j - p_{pj} - k_j p_{pj} = a_3 \frac{dp_{pj}}{d\theta} \tag{3}$$

$$t_j - t_{pj} + \beta k_j p_{pj} = a_4 \frac{dt_{pj}}{d\theta} \tag{4}$$

where

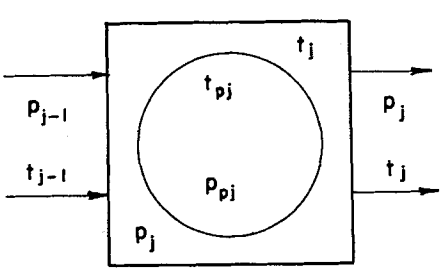

Fig. 1. Schematic of a simple cell.

$$M = \frac{G}{P\bar{m}\, k_g\, a_v\, \eta D_p} = \frac{H_g}{\eta D_p}, \quad k_j = \frac{D_p}{6}\frac{\rho_s S_g k'_j}{k_g} \tag{5}$$

$$H = \frac{Gc_f}{h_f\, a_v\, \eta D_p} = \frac{H_T}{\eta D_p}, \quad \beta = \frac{k_g}{h_f}(-\Delta H)$$

$$a_1 = \frac{\epsilon\rho_f}{k_g\, a_v\, P\bar{m}}, \quad a_2 = \frac{\epsilon\rho_f c_f}{a_v h_f}$$

$$a_3 = \frac{D_p}{6}\frac{\alpha\,\rho_{fp}}{\bar{m}\, k_g}, \quad a_4 = \frac{D_p}{6}\frac{\rho_s c_s}{h_f}$$

subject to the inlet conditions

$$\begin{aligned} t_e &= t_e(\theta) \\ p_e &= p_e(\theta) \end{aligned} \tag{6}$$

and to the initial conditions

$$\left.\begin{aligned} p_j &= p_{j0} \\ t_j &= t_{j0} \\ p_{pj} &= p_{pj0} \\ t_{pj} &= t_{pj0} \end{aligned}\right\} \quad \theta = 0,\ j = 1, 2, \ldots, n \tag{7}$$

STEADY STATE DETERMINATION

The steady state equations are:

$$M(p_{j-1} - p_j) = p_j - p_{pj} \tag{8}$$

$$H(t_{j-1} - t_j) = t_j - t_{pj} \tag{9}$$

$$p_j - p_{pj} = k_j p_{pj} \tag{10}$$

$$t_j - t_{pj} = \beta k_j p_{pj} \tag{11}$$

where k_j is of the form

$$k_j = k_0 \exp(-\Delta E/Rt_{pj})$$

By summing the first j equations an overall energy balance is obtained:

$$H(t_j - t_e) = \beta M(p_e - p_j) \tag{12}$$

We define $t_{\max}$ to be the temperature for which $p_j = 0$ to obtain

$$H(t_{\max} - t_e) = \beta M p_e \tag{13}$$

then Equations (12) and (13) can be combined to give

$$H(t_{\max} - t_j) = \beta M p_j \tag{14}$$

Equations (10) and (11) can be used to eliminate p_{pj} and by use of Equation (14) one obtains, exactly as for the continuous model, the condition

$$Q_I = \frac{M(t_{pj} - t_j)}{H(t_{\max} - t_j)} = \delta_j = Q_{II} \tag{15}$$

where

$$\delta_j = \frac{k_j}{1 + k_j}$$

Equation (15) enables one to determine the possible values of t_{pj} for a given value of t_j from the intersections between the Q_I and Q_{II} curves. It has already been shown (5) that all the straight lines Q_I pass through a common point, S, at $t_j = t_{\max}$ for which $Q_I = M/H$.

In order to determine graphically the change of temperature with j the following method can be used. Equation (9) can be rearranged to read

$$\frac{H}{H+1}(t_{pj} - t_{j-1}) = t_{pj} - t_j \tag{16}$$

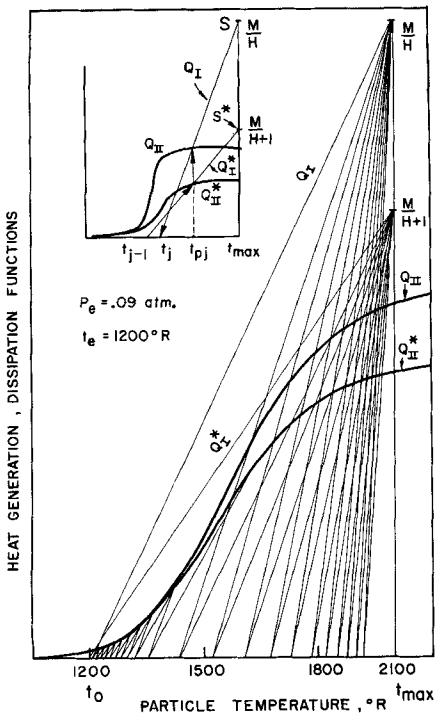

Fig. 2. Use of a graphical marching technique to determine the steady state profile.

By writing Equation (14) for j and $j-1$ one obtains

$$\frac{t_{\max}-t_j}{t_{\max}-t_{j-1}}=\frac{p_j}{p_{j-1}}=\frac{M}{M+\delta_j} \tag{17}$$

Thus, by multiplying Equation (15) by $M(M+\delta_j)^{-1}$ and use of Equations (16) and (17) one obtains

$$Q_I^*=\frac{M}{H+1}\frac{t_{pj}-t_{j-1}}{t_{\max}-t_{j-1}}=\frac{M\delta_j}{M+\delta_j}=Q_{II}^* \tag{18}$$

Thus, all the Q_I^* lines must pass through a common point S^* for which $t_p=t_{\max}$ and $Q_I^*=\dfrac{M}{H+1}$.

A simultaneous use of the Q_I and Q_{II} curves with the Q_I^* and Q_{II}^* curves enables one to determine the temperature profile by the following graphical marching technique. (See Figure 2).

1. For a given t_{j-1} determine by use of the Q_I^* and Q_{II}^* curves the value of t_{pj}, say b.
2. Determine from the Q_{II} curve the value of δ_j for $t_{pj}=b$, say c.
3. Draw a straight Q_I line through the points S and c, to determine the value of t_j.

When multiple intersections occur between the Q_I and Q_{II} curves this procedure can be used to determine all the possible steady states. However, transient computations are necessary to determine which of these possible steady states will be obtained from a given initial condition. Stability considerations can be used to reduce the number of possible steady states.

STABILITY ANALYSIS

For the continuous model (5) necessary and sufficient conditions for stability of each particle in the bed which neglect the effect of disturbances in the gas are

$$1+k_j-\beta\gamma_j k_j>0 \tag{19}$$

where

$$\gamma_j=p_{pj}\frac{\Delta E}{Rt_{pj}^2}$$

and

$$\frac{H\rho_s c_s}{M\rho_f c_f \alpha \delta_j}>1 \tag{20}$$

Condition (19) can be rewritten as

$$\frac{dQ_I}{dt_{pj}}>\frac{dQ_{II}}{dt_{pj}} \tag{21}$$

and condition (20) is usually implied by the slope condition (21) for gas-solid systems.

With the cell model one can determine necessary and sufficient conditions for stability of the whole bed including the gas. Let us define

$$\begin{aligned} x_j&=p_j-p_{js}\\ y_j&=t_j-t_{js}\\ w_j&=p_{pj}-p_{pjs}\\ z_j&=t_{pj}-t_{pjs} \end{aligned} \tag{22}$$

where the subscript s denotes steady state conditions.

By linearizing the transient Equations (1) to (4) around the steady state one obtains

$$\mathbf{C}\frac{d\mathbf{X}}{d\theta}=\mathbf{B}\,\mathbf{X} \tag{23}$$

where

$$X^T=[x_1, y_1, w_1, z_1; \ldots; x_n, y_n, w_n, z_n]$$

$$\mathbf{B}=\begin{bmatrix} \mathbf{A}_1 & 0 & \cdots & 0\\ \mathbf{D} & \mathbf{A}_2 & 0 & \vdots\\ 0 & \mathbf{D} & \mathbf{A}_3 & 0\\ \vdots & & \ddots & \vdots\\ 0 & \cdots & 0 & \mathbf{D}\ \ \mathbf{A}_n \end{bmatrix}$$

$$\mathbf{C}=\begin{bmatrix} \mathbf{a} & 0 & \cdots & 0\\ 0 & \mathbf{a} & \cdots & 0\\ \vdots & & & \vdots\\ 0 & \cdots & 0 & \mathbf{a} \end{bmatrix}$$

$$;\quad \mathbf{a}=\begin{bmatrix} a_1 & 0 & 0 & 0\\ 0 & a_2 & 0 & 0\\ 0 & 0 & a_3 & 0\\ 0 & 0 & 0 & a_4 \end{bmatrix}$$

$$\mathbf{A}_j=\begin{bmatrix} -(1+M) & 0 & 1 & 0\\ 0 & -(1+H) & 0 & 1\\ 1 & 0 & -(1+k_j) & -\gamma_j k_j\\ 0 & 1 & \beta k_j & -(1-\gamma_j\beta k_j) \end{bmatrix}$$

$$\mathbf{D}=\begin{bmatrix} M & 0 & 0 & 0\\ 0 & H & 0 & 0\\ 0 & 0 & 0 & 0\\ 0 & 0 & 0 & 0 \end{bmatrix} \tag{24}$$

A necessary and sufficient condition for stability is that all the eigenvalues of

$$\det(\mathbf{C}^{-1}\mathbf{B}-\lambda\mathbf{I})=0 \tag{25}$$

have negative real parts. Due to the special form of the matrices $\mathbf{B}$ and $\mathbf{C}$, Equation (25) can be rewritten as

$$\prod_{j=1}^{n} \det\left(\mathbf{a}^{-1}\mathbf{A}_j - \lambda\mathbf{I}\right) =$$

$$\prod_{j=1}^{n} \left(\lambda^4 + b_{j1}\lambda^3 + b_{j2}\lambda^2 + b_{j3}\lambda + b_{j4}\right) = 0 \quad (26)$$

where

$$b_{j1} = \frac{1+M}{a_1} + \frac{1+H}{a_2} + \frac{1}{a_3} + \frac{1}{a_4}\left(1 + \frac{a_4}{a_3}k_j - \beta\gamma_j k_j\right) \quad (27)$$

$$b_{j2} = \frac{1 + k_j - \beta\gamma_j k_j}{a_3 a_4} + \frac{1+M}{a_1 a_3}\left[\left(1 + k_j - \frac{a_3}{a_4}\beta\gamma_j k_j\right)\cdot\left(1 + \frac{(1+H)a_1}{(1+M)a_2}\right) - \frac{1}{1+M} + \frac{a_3}{a_4} + \frac{(1+H)a_3}{a_2}\right] + \frac{H}{a_2 a_4} \quad (28)$$

$$b_{j3} = (1 + k_j - \gamma_j\beta k_j)\left(\frac{H}{a_2 a_3 a_4} + \frac{M}{a_1 a_3 a_4}\right) + \frac{k_j}{a_1 a_3 a_4} - \frac{\beta\gamma_j k_j}{a_2 a_3 a_4} + \frac{M(1+H) - \frac{a_3}{a_4}(1+M)}{a_1 a_2 a_3} + \frac{(1+M)(1+H)}{a_1 a_2 a_3}\left(1 + \frac{a_4}{a_3}k_j - \beta\gamma_j k_j\right) \quad (29)$$

$$b_{j4} = \frac{1}{a_1 a_2 a_3 a_4}\{[H(1+k_j)M + k_j] - (H+1)M\beta\gamma_j k_j\} \quad (30)$$

According to the Lienard-Chipart criterion (3) the eigenvalues of Equation (26) will have negative parts if, and only if

$$b_{j1} > 0 \quad (31)$$

$$b_{j2} > 0 \quad (32)$$

$$b_{j1} b_{j2} b_{j3} > b^2_{j1} b_{j4} + b^2_{j3} \quad (33)$$

$$b_{j4} > 0 \quad (34)$$

$$j = 1, 2, \ldots, n$$

For gas-solid systems $a_4/a_3 >> 1$. Hence it can be easily seen that if the slope condition (19) is satisfied, so are conditions (31) and (32). If the values of the b_{ji}'s are substituted into condition (33) an extremely complicated expression is obtained. It was not possible to show that the other conditions imply that this condition holds in practice.

Condition (34) can be rewritten as

$$\frac{1}{\beta p_{pj}} > \frac{H+1}{H}\frac{\Delta E}{Rt^2_{pj}}\frac{k_j M}{M(1+k_j) + k_j} \quad (35)$$

It is easily verified that condition (35) can be rewritten as

$$\frac{1}{\beta p_{pj}} > \frac{H+1}{H}\left(\frac{M}{M+\delta_j}\right)^3 \frac{d\delta_j}{dt_{pj}} \quad (36)$$

or as

$$\frac{dQ_I}{dt_{pj}} > \frac{H+1}{H}\left(\frac{M}{M+\delta_j}\right)^3 \frac{dQ_{II}}{dt_{pj}} \quad (37)$$

If

$$\frac{H+1}{H}\left(\frac{M}{M+\delta_j}\right)^3 > 1 \quad (38)$$

then condition (37) is stronger than the slope condition (21). M and H are usually of order one, while δ_j is always smaller than one. Thus, condition (38) is usually satisfied at low temperatures for which $\delta_j << 1$. At high temperatures for which $\delta_j \approx 1$ condition (38) is usually not satisfied and the slope condition (37) is no longer sufficient for stability. If condition (38) is not satisfied the slope condition is stronger than the condition (37). Thus, the coupling effect of the flow of the gas stabilizes the bed. However, if condition (38) is satisfied, the gas flow tends to destabilize the bed.

NUMERICAL SOLUTION OF TRANSIENT EQUATIONS

For the case in which there are three intersections between the Q_I and Q_{II} curves, one must solve numerically the transient equations to determine which of the possible steady states will be obtained.

One of the important advantages of the cell model, if it is applicable, is that the transient equations can be solved faster than for the continuous model used earlier (5), since computations are by a straightforward marching technique while the cell model requires a more complicated method. A comparison between the two models showed that use of the cell model reduces the time of computation by a factor of about twenty with the same method of integration. The time of computation on a C.D.C. 1604 was about one-twentieth of real time and use of the C.D.C. 6600 reduced this time by another factor of twenty.

For purposes of comparison the same numerical example considered for the continuous model was solved. In terms of the dimensionless groups the system parameters were

$$k_j = \exp\left[12.98 - 22{,}000/t_{pj}\right]$$
$$\beta = 6{,}000\ ^\circ\text{F./atm.}$$

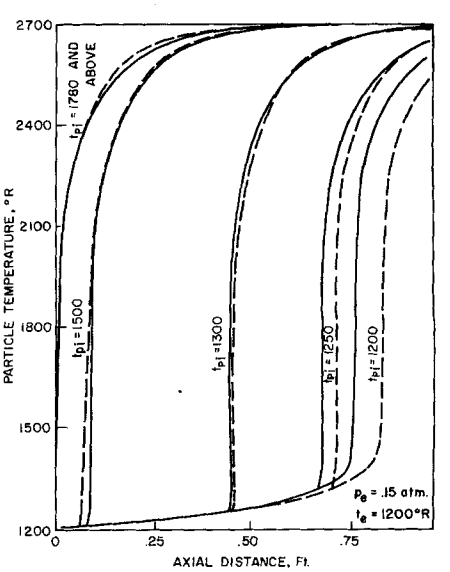

Fig. 3. Effect of initial temperature on the steady state temperature profiles (solid curve) cell model, (broken lines) continuous model.

$$H = 2.352$$
$$M = 3.919$$
$$M/H = 1.67$$
$$a_4 = 1/5.45 \text{ min.} \qquad (39)$$

Although the cell thickness was taken as $\sqrt{2/3}\ D_p$ computations have shown that a 100% increase or decrease in the size of a cell has an almost negligible effect on the position of the steady state profiles.

Figure 3 shows a comparison of the various initial bed temperatures on the position of the reaction zone as computed by the cell and continuous models. It is noted that both models predict the same profiles for high initial temperatures for which the reaction zone is near the inlet of the bed. As the initial temperature is reduced the reaction zones move downstream. For these cases the cell model predicts that the reaction zone will be nearer to the inlet of the bed. A similar effect was noted earlier (*7*) when axial diffusion was included in the continuous model.

EFFECTS OF CHANGES IN THE GAS VELOCITY

According to Wicke (*11*) the transfer coefficients in the bed are a function of $Re^{0.6}$, while the height of a transfer unit is a function of $Re^{0.4}$. If we denote by u_o the velocity of the gas for the standard example parameters, then changing the velocity to u will affect the parameters in the following way

$$H = 2.352 \left(\frac{u}{u_o}\right)^{0.4}$$

$$M = \frac{3.919\,H}{2.352}$$

$$k_j = \left(\frac{2.352}{H}\right)^{1.5} \exp\left[12.98 - 22{,}000/t_{pj}\right]$$

$$a_4 = \frac{1}{5.45}\left(\frac{2.352}{H}\right)^{1.5} \qquad (40)$$

Thus, instead of specifying the changes in the value of the velocity, it is sufficient to define the resulting change in the values of H.

A variation of the velocity affects the shape of the Q_{II} and Q_{II}^* curves and the location of the S^* point. However, it does not affect the position of the S point, since the value of M/H is independent of variations in the gas velocity. Thus, it is clear that changes in the gas velocity may have a very important effect on the profiles of the various possible steady states.

Figure 4 describes the simplest possible case where each particle has a unique state in the given range of

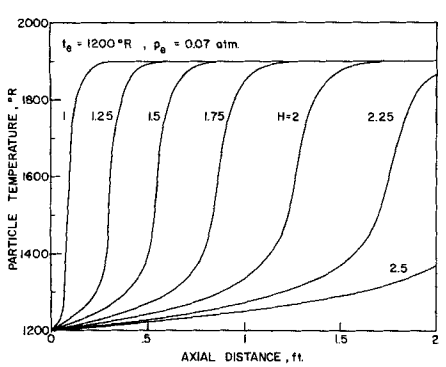

Fig. 4. Effect of different gas velocities (different values of H) on the steady state profiles for the case that each particle has a unique steady state.

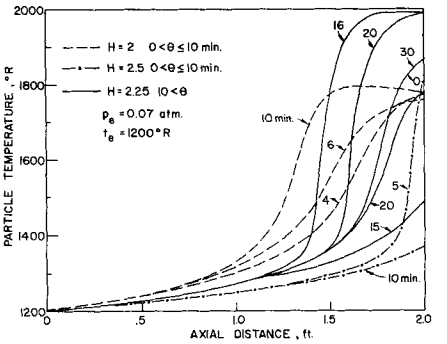

Fig. 5. Transient temperature profiles due to variation of gas velocities (changes in H) for a case in which all particles have a unique state.

velocities. In this case the graphical procedure illustrated in Figure 2 can be used to determine the steady state profiles. Low velocities (low values of H) shift the reaction zone towards the inlet of the bed, while high velocities shift the reaction zone out of the reactor causing a blow out.

Figure 5 shows transient changes in the temperature profile due to a disturbance which lasted 10 min. in the gas velocity (shown by changes in H). It is seen that as the velocity is decreased (H changes from 2.25 to 2) the reaction zone moves towards the inlet of the bed. As the velocity is changed back to the original value the reaction zone returns to its original value as expected. As the velocity is increased the reaction zone is blown out of the bed and when the original value of the velocity is restored, so is the position of the reaction zone. Thus, for this case the transient disturbances in the flow velocity do not affect the final steady state.

An important transient phenomenon is that as the reaction zone moves downstream (see curves for 16 and 20 min.) the maximum temperature exceeds the maximum steady state temperature rise by more than 100 deg. This phenomenon may be important if the catalyst is sensitive to high temperatures. Such transients have been observed experimentally by Wicke and coworkers (*9* to *12*).

A more complicated case occurs when some of the particles have nonunique steady states for the given range or velocities. As was shown in Figure 3 under such conditions the reaction zone may occur anywhere in a certain range with the initial conditions determining the location of the reaction zone. Thus a temperature profile could be one of the many possible steady state profiles that arise from various velocities and initial temperatures. This condition is demonstrated in Figure 6 in which steady state profiles for various velocities (values of H) and two different initial temperatures are shown. Note that the temperature profile for $H = 3.25$ and $t_{pi} = 1{,}200°\text{R}$. is very close to that of $H = 4$, $t_{pi} = 1{,}500°\text{R}$. Thus, changes in the velocity of the gas may or may not cause a shift in the position of the reaction zone. Moreover, as will be shown later, the effect of velocity may be irreversible. For example, a decrease in the velocity may shift the reaction zone downstream, while an increase in the velocity may not affect its position. The opposite effect may also occur.

It is seen from Figure 6 that an increase in the initial temperature tends to decrease the range of velocities for which the reaction zose is not shifted towards the inlet or blown out. For $t_{pi} = 1{,}200°\text{R}$. this occurs for $1.5 < H < 3.25$, while for $t_{pi} = 1{,}500°\text{R}$. this occurs for $3 < H < 4$.

Figure 7 shows the effect of variation in the velocity of the gas on one of the possible steady states shown in Figure 3. In both cases the velocity was changed from its steady state value and then restored to its original value.

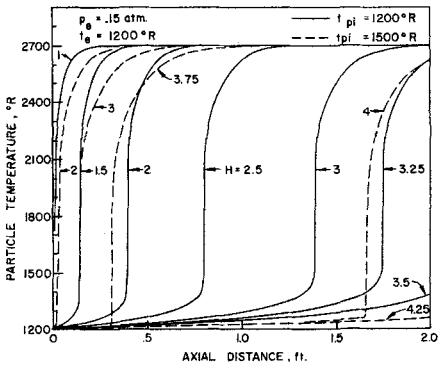

Fig. 6. Effect of initial temperature and gas velocity on the steady state temperature profile for a case in which all particles have a unique state.

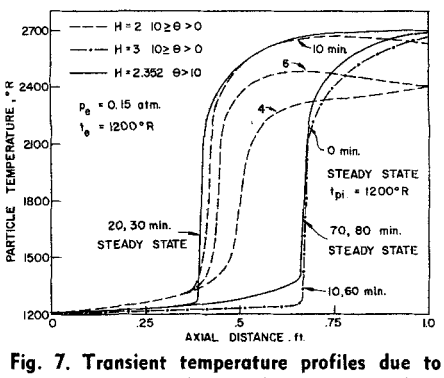

Fig. 7. Transient temperature profiles due to variation of gas velocities for a case in which some particles have a nonunique state.

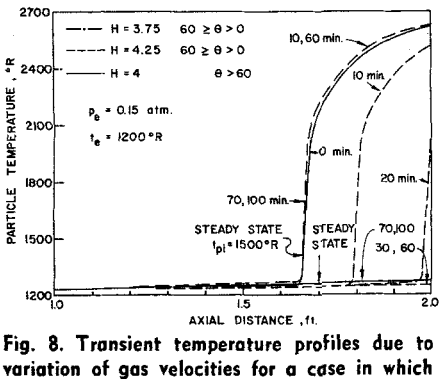

Fig. 8. Transient temperature profiles due to variation of gas velocities for a case in which some particles have a nonunique state.

It is seen that as the velocity is decreased (H changes from 2.352 to 2) the reaction zone moves upstream. As the velocity is restored to the original value, the reaction zone remains in the new position and does not move backwards. However, an increase in the velocity so that H changes from 2.352 to 3 does not change the position of the reaction zone. As the original value of the velocity is restored ($H = 2.352$) the original steady state profile is obtained. It is clear that for such a case small random fluctuations around the average velocity may move the reaction zone towards the inlet of the bed.

Figure 8 shows a case in which an increase in the velocity shifts the reaction zone downstream until blowout occurs. However, a decrease in the velocity does not shift the reaction zone upstream. Hence, when the velocity was restored to the steady state value, the original profile was obtained. For such a case small fluctuations around the average velocity might shift the reaction zone out of the bed.

COUPLED CELL MODELS

In the previous model it was assumed that the transport of energy between the catalyst particles was only through the medium of the external fluid which moves only in the downstream direction. In this section we will determine the effect of coupling between catalyst particles on the steady state profiles. Physically such coupling may occur geometrically; that is, the front and back of the particles form the boundaries of two different successive cells, or from energy feedback in the form of radiation.

In geometric coupling one half of the external area of the catalyst particles is assigned to each of the mixing pockets that contact it. A schematic diagram of the model is shown in Figure 9.

With the small capacitance terms a_1 a_2 a_3 neglected the system of equations is

$$M(p_{j-1} - p_j) - \left(p_j - \frac{p_{pj} + p_{p,j+1}}{2}\right) = 0 \qquad (41)$$

$$H(t_{j-1} - t_j) - \left(t_j - \frac{t_{pj} + t_{p,j+1}}{2}\right) = 0 \qquad (42)$$

$$\frac{p_{j-1} + p_j}{2} - (1 + k_j)\, p_{pj} = 0 \qquad (43)$$

$$\frac{t_{j+1} + t_j}{2} - t_{pj} + \beta k_j p_{pj} = a_4 \frac{dt_p}{d\theta} \qquad (44)$$

$j = 1, 2, \ldots, n$

For $j = 0$

$$p_j = p_e$$
$$t_j = t_e$$

and, by convention, let

$$p_{p,N+1} = p_{pN}$$
$$t_{p,N+1} = t_{pN} \qquad (45)$$

There is also the initial condition:

$$t_{pj}(0) = t_{pjI}$$

The system appears to be quite similar to that of the uncoupled model. However, it can be shown that a backmixing effect is induced by the coupling.

Define

$$\bar{t}_j = \frac{t_{j-1} + t_j}{2} \qquad (46)$$

$$\bar{p}_j = \frac{p_{j-1} + p_j}{2} \qquad (47)$$

In exactly the same way as Equation (15) was derived one can obtain in this case the relation

$$Q_I = \frac{M}{H}\frac{t_{pj} - \bar{t}_j}{\bar{t}_{\max} - \bar{t}_j} = \delta_j \qquad (48)$$

where $\bar{t}_{\max}$ occurs when $\bar{p}_j = 0$.

The graphical analysis for this case is the same as for the first uncoupled cell model except that an average value of interstitial fluid temperature is the intercept on the t_{pj} axis.

Multiple steady state solutions can be shown to exist for a range of values of the intercept $\bar{t}_j$. Because of the coupling, however, it is not possible to extend the analysis to obtain a second graphical solution. Consequently, there is no marching graphical development of the steady state profiles.

A simple perturbation in the particle variables alone gives the already familiar criterion for stability:

$$p_{pj}\left(\frac{\beta\,\Delta E}{Rt^2_{pj}}\right)\frac{k_j}{1 + k_j} < 1 \qquad (49)$$

for the steady state.

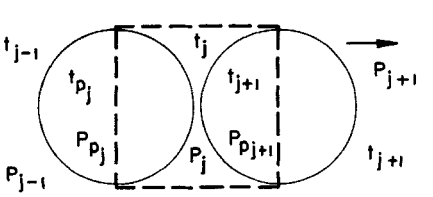

Fig. 9. A Schematic of a cell with geometric coupling.

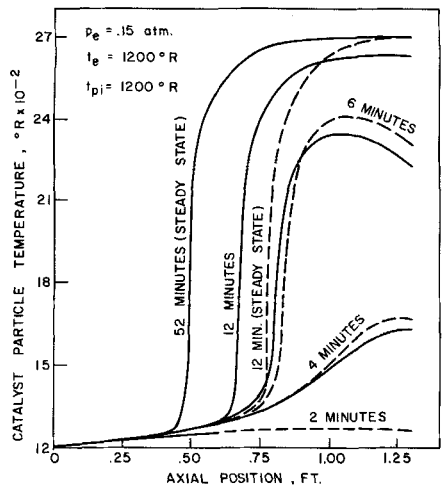

Fig. 10. The transient behavior of a coupled cell model (solid curves) compared to that of the uncoupled cell model (broken lines).

When Equation (49) is combined with Equation (42), one obtains after regrouping

$$\left(\beta \frac{p_{j-1} + p_j}{2}\right)^{-1} > \frac{d\delta_j}{dt_{pj}} \tag{50}$$

This is readily interpretable as the slope condition for the graphical analysis of the previous section.

If all the variables in the system are perturbed, a complex stability matrix is obtained, this leads to extremely complicated algebraic expression that do not have a simple physical meaning, and do not uncover new information of a general nature. In general the feedback of heat and the forward feed of reactants should have an opposing effect on the stability of the bed.

Several examples were investigated numerically to find the basic characteristics of this geometrically coupled model. Figure 10 compares the transient behavior of the coupled cell model with that of the uncoupled cell. It can be seen that the steady state for the coupled cell is further upstream and is established much slower than the steady state for the uncoupled cell model. During the transient period one can note the occurrence of a temperature profile which slowly creeps towards the inlet. This behavior is characteristic of all coupled models.

Figure 11 shows the effect of the initial temperature on the final steady state profiles for a case identical to that shown in the example of Figure 3. The coupled model predicts that the reaction zone occurs further upstream than does the uncoupled model. Furthermore the coupled model predicts that the zone in which multiple steady states may occur is much smaller than that predicted by the simple model.

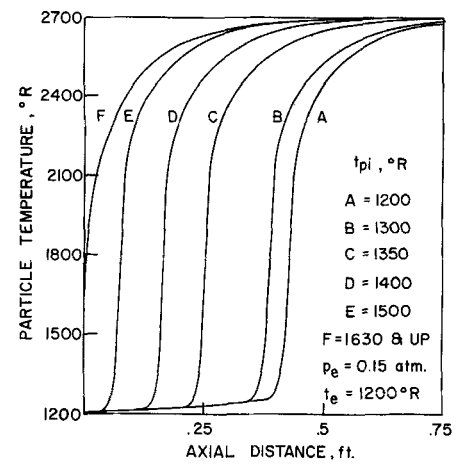

Fig. 11. Effect of initial bed temperature on the steady state profiles, coupled model.

The effect of changing the velocity was exactly the same as that found for the uncoupled cell, except that the response time was somewhat slower.

We consider now a model in which the catalyst particles are coupled by radiation. The sighting factor will be assumed independent of position and the emissivity to be independent of temperature. The last assumption is somewhat doubtful and Chen and Churchill (*1*) reported this property to depend on the type of packing. When specific data is available it can be easily programmed into the model. It is also assumed that the gas does not adsorb radiation energy.

Under these conditions the radiation affects only the energy conservation equation of the cell, which has the form

$$t_j - t_{pj} + \beta k_j p_{pj} + r(t^4_{p,j+1} + t^4_{p,j+1} - 2t^4_{pj}) = a_4 \frac{dt_{pj}}{d\theta} \tag{51}$$

$$r = \frac{\epsilon' F \sigma}{2 h_f}$$

The steady state equation for a given cell, j, becomes

$$\frac{t_{pj} - t_j - r(t^4_{p,j+1} + t^4_{p,j-1} - 2t^4_{pj})}{\frac{H}{M}(t_e - t_j) + \beta p_e + \frac{r}{M}(t^4_{p,j+1} - t^4_{pj})} = \delta_j \tag{52}$$

Due to instantaneous transfer of radiation any change in the assumed value of t_{pj} will affect both $t_{p,j-1}$ and $t_{p,j+1}$. No simple graphical procedure to determine the steady state is possible, therefore, the steady states have to be determined by a numerical procedure.

In this case an asymptotic stability analysis of only one particle is useless since an instantaneous transport mechanism is included in the model, and the effect of perturbing the whole bed yields extremely complex algebraic conditions with no simple physical meaning. Thus, no general information can be obtained in this way. The only apparant method for checking the stability of a given steady state is by solving the transient equations.

It was found that the effect of radiation is to shift the reaction zone upstream and to increase the time required to reach a steady state. Figure 12 shows a typical transient behavior. After an induction period a temperature profile of almost constant shape is established which slowly creeps upstream until a steady state is obtained. In this example the steady state is established near the inlet of the bed. It should be noted that the maximum temperature of the uptream creeping reaction zone is lower than that of the steady state maximum temperature. This phenomenon has been observed and explained by Wicke

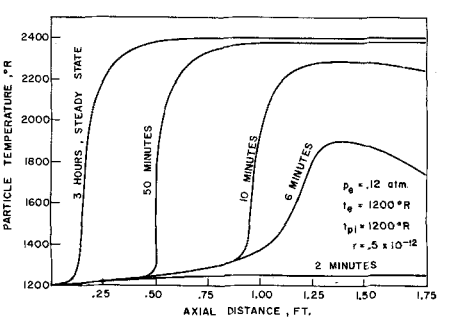

Fig. 12. Development of a steady state profile for a cell model coupled by radiation.

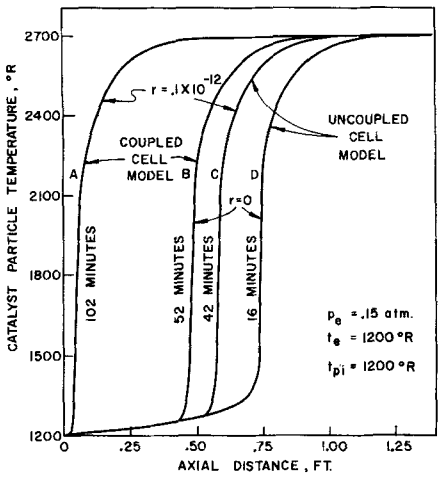

Fig. 13. The effect of increasing cellular interaction on the final steady state profiles and the time required to reach them.

(*11*). The occurrence of creeping profiles has also been reported by Frank Kamenetskii (*4*, p. 347) for the catalytic oxidation of isopropyl alcohol.

Figure 13 shows the effect of increasing cellular coupling on the position of the reaction zone. Curves *A* and *B* in this figure are for combined geometric and radiative coupling while *C* and *D* were obtained for the case with no geometric coupling. The more pronounced the coupling the more the reaction zone is shifted toward the bed inlet and the longer is the transient period.

CONCLUSIONS

1. A simple cell model was developed which enabled the determination of necessary and sufficient conditions for the stability of the whole bed. These conditions are different from those obtained by considering only the effect of perturbing a single particle.

2. The effect of flow variation on the position of the reaction zone has been investigated. Under certain conditions this effect may be irreversible, that is, a decrease in the velocity may shift the reaction zone upstream, while an increase in the velocity will not affect the position of the reaction zone. The opposite effect may also occur.

3. The effect of coupling between the particles by means of a geometric structure or heat transfer by radiation has been investigated. It was found that increasing the cellular coupling tends to shift the reaction zone upstream, increase the time of the transient behavior, decrease the zone in which multiple steady states can exist, and cause the appearance of creeping profiles.

ACKNOWLEDGMENT

This work was supported by the National Science Foundation.

NOTATION

a_1,a_2,a_3,a_4 = capacity terms defined by Equation (5)
a_v = total surface area of particles per unit volume of bed
A,B,C = matrices defined by Equation (24)
c_f = specific heat of gas mixture
c_s = specific heat of particle
D = matrix defined by Equation (24)
D_p = particle diameter
ΔE = activation energy
F = geometric sighting factor
G = fluid mass velocity
H = ratio of $H_h/D_p\eta$ (dimensionless)
H_g = *HTU* for mass transfer
H_h = *HTU* for heat transfer
ΔH = heat of reaction
h_f = film heat transfer coefficient
k = dimensionless reaction rate
k_g = mass transfer coefficient
k' = reaction rate coefficient
M = ratio of $H_g/\eta D_p$
m = average molecular weight of gas mixture
P = total pressure
p = partial pressure of reactant in gas
p_p = partial pressure of reactant in catalyst
p_{pi} = initial partial pressure of reactant in catalyst
Q_I = heat dissipation function
Q_{II} = heat generation function
R = ideal gas law constant
r' = radiation parameter
r = $10^{12}\ r'$
S_g = surface area of catalyst per unit mass of catalyst
t = gas temperature
t_{max} = maximum temperature defined by Equation (13)
t_p = particle temperature
u = fluid velocity
X = vector defined by Equation (24)

Greek Letters

α = void fraction of particle
β = $(-\Delta H)\ k_g/h_f$
γ = $p_p\ \Delta E/Rt_p^2$
δ = heat generation function, $k/1 + k$
ϵ = fractional void volume of bed
ϵ' = emissivity of the catalyst particle
η = height of cell/D_p
θ = time
λ = eigenvalue
ρ_f = density of fluid
ρ_{fp} = density of fluid in particle
ρ_s = density of solid
σ = Stephan Boltzman constant

Subscripts

e = influent conditions
i = initial conditions
j = denotes cell number
s = steady state conditions

LITERATURE CITED

1. Chen, J. C., and S. W. Churchill, *AIChE J.*, **9**, 35 (1963).
2. Deans, H. A., and Leon Lapidus, *ibid.*, **6**, 656 (1960).
3. Gautmacher, F. R., "Application of the Theory of Matrices," Interscience, New York (1959).
4. Frank Kamenetskii, D. A., "Diffusion and Heat Exchange in Chemical Kinetics," Princeton Univ. Press, New Jersey (1955).
5. Liu, S. L., and N. R. Amundson, *Ind. Eng. Chem. Fundamentals*, **1**, 200 (1962).
6. ———, R. Aris, and N. R. Amundson, *ibid.*, **2**, 12 (1963).
7. Liu, S. L., and N. R. Amundson, *ibid.*, **2**, 183 (1963).
8. McGuire, M. L., and Leon Lapidus, *AIChE J.*, **2**, 82 (1965).
9. Wicke, E., and D. Vortmeyer, *Z. Electrochem.*, **63**, 145 (1959).
10. Wicke, E., *ibid.*, **65**, 267 (1961).
11. ———, *Chem. Ing. Tech.*, **37**, 892 (1965).
12. ———, and G. Padberg, *Chem. Eng. Sci.*, **22**, 1035 (1967).

Manuscript received September 29, 1967; revision received October 26, 1967; paper accepted October 27, 1967. Paper presented at AIChE St. Louis Meeting.